Citation: CPT Pharmacometrics Syst. Pharmacol. (2017) 6, 249–257; doi:10.1002/psp4.12160

ORIGINAL ARTICLE

Population Pharmacokinetics and Pharmacodynamics of Benralizumab in Healthy Volunteers and Patients With Asthma

B Wang[1]*, L Yan[1], Z Yao[1,2] and LK Roskos[3]

Benralizumab is a humanized, afucosylated, anti-interleukin-5 receptor α, immunoglobulin G (IgG) $_1$ κ monoclonal antibody. We developed a population pharmacokinetic (PK)/pharmacodynamic (PD) model for benralizumab by analyzing PK and blood eosinophil count data from two healthy volunteer studies ($N = 48$) and four studies in patients with asthma ($N = 152$). Benralizumab PK was dose-proportional and adequately described by a two-compartment model with first-order elimination from the central compartment and first-order absorption from the subcutaneous dosing site. The estimated systemic clearance and volume of distribution were typical for human IgG. Body weight and high-titer antidrug antibodies were identified as relevant covariates influencing the PK of benralizumab. Depletion of blood eosinophil counts was depicted by a modified transit model in which benralizumab induced depletion of eosinophils in each age compartment. Stochastic simulations supported an every-8-week dosing schedule of benralizumab for a phase IIb study in patients with uncontrolled asthma.

CPT Pharmacometrics Syst. Pharmacol. (2017) **6**, 249–257; doi:10.1002/psp4.12160; published online 21 January 2017.

Study Highlights

WHAT IS THE CURRENT KNOWLEDGE ON THE TOPIC?

☑ Benralizumab, a humanized, afucosylated anti-IL-5Rα mAb, depleted blood and airway eosinophils, and improved asthma control in phase II studies.

WHAT QUESTION DID THIS STUDY ADDRESS?

☑ A population approach characterized the PK/PD properties of benralizumab with data from six early-stage clinical studies in healthy volunteers and patients with asthma.

WHAT THIS STUDY ADDS TO OUR KNOWLEDGE

☑ Unlike other cell membrane receptor-targeted mAbs, benralizumab PK is dose-proportional (0.03–3 mg/kg i.v.; 25–200 mg s.c.), and typical for IgG as a result of rapid depletion of IL-5R-expressing eosinophils. Benralizumab administration resulted in substantial and prolonged suppression of blood eosinophil count because of enhanced ADCC activity. Stochastic simulations supported selection of three dosages and every-8-week dosing for a proof-of-concept, phase IIb study.

HOW MIGHT THIS CHANGE DRUG DISCOVERY, DEVELOPMENT, AND/OR THERAPEUTICS?

☑ Population meta-analyses of merged data from small, early-stage studies enables better characterization of PK/PD properties of candidate drugs, identification of covariate effects, and rational selection of dosage regimens for future studies.

Interleukin-5 (IL-5) is a cytokine involved in regulating the differentiation, proliferation, and activation of eosinophils via the human IL-5 receptor (IL-5R).[1,2] The α-chain of IL-5R exclusively binds to IL-5, and its expression is restricted largely to eosinophils and basophils in humans.[3–5] Eosinophils play a key role in the pathophysiology of asthma disorders by releasing a wide range of mediators, cytokines, and growth factors.[6,7] The IL-5R system provides a selective anti-eosinophil approach that may be beneficial in asthma.[8] Benralizumab is an investigational, humanized, afucosylated, anti-IL-5Rα, immunoglobulin G_1 κ (IgG_1 κ) monoclonal antibody (mAb).[9] Afucosylation of benralizumab increases its ability to bind to human FcγRIIIa, the main Fc receptors expressed on natural killer cells, macrophages, and neutrophils. Thus, upon binding to IL-5Rα, benralizumab activates effector cells leading to antibody-dependent cell-mediated cytotoxicity (ADCC), resulting in the apoptosis of eosinophils.[10]

Benralizumab pharmacokinetics (PKs) were evaluated following i.v. administration in a single-ascending-dose study (0.0003–3 mg/kg) in patients with mild atopic asthma.[11] The PK of benralizumab was dose-proportional over a wide dosing range (0.03–3 mg/kg), with an elimination half-life (18 days) and volume of distribution (52–93 mL/kg) consistent with an IgG antibody. Benralizumab was well tolerated and reduced blood eosinophil counts at dosages of ≥0.3 mg/kg; these eosinophil count reductions lasted for at least 12 weeks. Currently, benralizumab is in phase III clinical development for the treatment of patients with severe, uncontrolled asthma with eosinophilic inflammation.[12]

To characterize the PK and pharmacodynamic (PD) properties of benralizumab in humans, benralizumab PK and

[1]MedImmune LLC, Mountain View, California, USA; [2]Current address: Janssen Research & Development, LLC, Spring House, Pennsylvania, USA; [3]MedImmune LLC, Gaithersburg, Maryland, USA. *Correspondence: B Wang (wangbi@medimmune.com)
Received 28 June 2016; accepted 13 November 2016; published online on 21 January 2017. doi:10.1002/psp4.12160

blood eosinophil count data from six early-stage studies (two single-dose studies in healthy volunteers in Japan and four clinical studies in adult patients with asthma in North America) were pooled and analyzed via a population approach. The model was subsequently used to aid the design of a phase IIb efficacy trial in patients with asthma.

METHODS

Study population and design

Benralizumab serum concentration and blood eosinophil count data from six clinical trials were included in the population PK and PK/PD analysis. The trials consisted of two phase I, single-ascending-dose studies in adult Japanese healthy volunteers with i.v. or s.c. administration and four North American studies in adult patients with asthma. In these studies, benralizumab doses ranged from 0.0003–3 mg/kg for the i.v. groups and 25–200 mg for the s.c. groups. Both single and repeat-dosage regimens were studied. The two studies in Japanese healthy volunteers provided an intensive sampling schedule to enrich the data in the pooled data set. The six studies provided a total of 1,820 serum benralizumab concentrations and 1,664 eosinophil counts from a total of 200 individuals.

All studies were conducted according to good clinical practice and followed the Declaration of Helsinki. Local ethics committees approved the study protocols and all amendments. Informed consent was obtained from all individuals.

Bioanalytical methodology

Two validated immunoassays were used to measure serum benralizumab concentrations. Two noncompeting antibenralizumab idiotype antibodies were used as the capturing and detecting reagents. For study MI-CP158, serum concentrations of benralizumab were measured with a validated enzyme linked immunoassay method that had a lower limit of quantitation of 60 ng/mL.[11] In this study, 12.3% of PK observations were recorded as below the lower limit of quantitation (BLQ). For the two Japanese studies and studies MI-CP166, MI-CP186, and MI-CP197, benralizumab was measured with a validated electrochemiluminescent sandwich immunoassay that used Meso Scale Discovery technology; the lower limit of quantitation was 3.86 ng/mL. In those studies, 12.6% of PK observations were recorded as BLQ.

Data analysis

PK and eosinophil data were analyzed with a nonlinear mixed effects modeling approach with the software package NONMEM (ICON Development Solutions, Hanover, MD; version 7.2). The first-order conditional estimation with interaction method was used to estimate benralizumab PK parameters; a Laplacian method was subsequently used to estimate parameters for PD modeling (IPP method).[13]

Pharmacokinetics model

A two-compartment model with first-order elimination from the central compartment and first-order absorption from the dosing site of s.c. administered benralizumab was evaluated as the structural model per prior analysis of phase I studies that used an intensive sampling scheme.[11] The two-compartment model was selected based upon goodness-of-fit plots and the likelihood objective function value. The absorption and disposition of benralizumab in humans are described by the following equations:

$$\frac{dA_{SC}}{dt} = -k_a \cdot A_{SC} \quad (1)$$

$$\frac{dC}{dt} = \frac{k_a \cdot F \cdot A_{SC}}{V_C} - \frac{CL \cdot C}{V_C} - \frac{Q}{V_C} \cdot (C - C_p) \quad (2)$$

$$\frac{dC_p}{dt} = \frac{Q}{V_p} \cdot (C - C_p) \quad (3)$$

A_{SC} represents the amount of administered benralizumab at the s.c. injection site. The benralizumab concentrations in the central and peripheral compartments are symbolized by C and C_p, respectively. CL represents the systemic clearance of benralizumab, and Q is the intercompartmental (distribution) clearance. V_c and V_p are the volumes of distribution of the central and peripheral compartments, respectively. The absorption of s.c. administered benralizumab is described by the first-order absorption rate constant (k_a) and bioavailability (F).

Interindividual variabilities (IIVs) were assumed to be log-normally distributed, $\theta_i = \theta_{TV} e^{\eta_i}$, where θ_i is the parameter for the i^{th} individual, θ_{TV} is the typical parameter value for the population and η_i is the random variable explaining the difference between the individual and the population; η_i was assumed to be normally distributed with a variance of ω^2. Residual variability was modeled with the assumption of additive and proportional components $Y_{ij} = C_{ij}(1 + \varepsilon_{ij1}) + \varepsilon_{ij2}$, where Y_{ij} is the observed serum concentration of the i^{th} individual at time j, and C_{ij} is the predicted concentration. Both ε_1 and ε_2 were assumed normally distributed with mean zero and estimated variances ω_1 and ω_2, respectively.

Pharmacokinetics covariate model

A forward addition process and a backward elimination process were used to evaluate continuous covariates, including baseline values of age, body weight, body mass index, and blood eosinophil count; and the categorical covariates of sex, race (white, Asian, black, and other), and smoking status. The presence of antidrug antibodies (ADAs) or high-titer ADA at each predesignated sampling visit was also evaluated as a potential categorical covariate on CL.

The relationship between continuous covariates and pharmacokinetic parameters (P) was modeled with nonlinear power functions (Eq. 4) with the covariate normalized to the population median for the dataset. The categorical covariates were modeled with the use of flag variables (1 and 0 for "true" and "false," respectively; Eq. 5). The potential effect of the presence of ADA was evaluated with a power function (Eq. 6), with IADA set to 0 for negative (absence) and 1 for positive (presence).

$$P = \theta_1 \cdot \left(\frac{Covariate}{Median\ Covariate}\right)^{\theta_2} \quad (4)$$

$$P = \theta_1 \cdot (Flag_1 + \theta_2 \cdot Flag_2 + \theta_3 \cdot Flag_3 \ldots) \quad (5)$$

$$P = \theta_1 \cdot e^{IADA \cdot \theta_2} \quad (6)$$

where the θs are the parameters to be estimated.

Demographic covariates were first explored by stepwise-generalized additive models to identify those with potential impact on PK structure parameters. In a sequential forward addition step, a covariate effect associated with $P \leq 0.05$ (Δobjective function value ≤ -3.8 with 1 degree of freedom) was included toward the development of a full covariate model. The full model was then subject to a more rigorous backward deletion procedure associated with $P < 0.001$ (Δobjective function value >10.8 when one covariate parameter was excluded), so the final PK model retained only those covariate effects with strong correlation with benralizumab PK.

Pharmacodynamics model

A hematopoietic transit model was developed to describe the blood eosinophil count data following benralizumab treatment.[14,15] The PD effect of benralizumab was exerted by asymptotic enhancement of eosinophil depletion in the blood, as the following differential equations demonstrate:

$$\frac{d\,Eos_1}{d\,t} = S_0 - \frac{n}{\Lambda} \cdot Eos_1 - \frac{E_{max} \cdot C}{EC_{50} + C} \cdot Eos_1 \quad (7)$$

$$\frac{d\,Eos_i}{d\,t} = \frac{n}{\Lambda} \cdot (Eos_{i-1} - Eos_i) - \frac{E_{max} \cdot C}{EC_{50} + C} \cdot Eos_i \quad (8)$$

In the above equations, Λ represents the longevity (lifespan) of blood eosinophils. E_{max} and EC_{50} are the maximum rate of eosinophil depletion by benralizumab and the serum concentration of benralizumab corresponding to half-maximal eosinophil depletion, respectively. The total blood eosinophil count, Eos_{total}, is calculated as the sum of eosinophils in all aging compartments: $Eos_{total} = \sum_{i=1}^{n} Eos_i$. The influx rate of eosinophils, S_0, is the ratio of Eos_{total} at time zero and Λ.

As for PK, the IIVs for PD parameters E_{max}, EC_{50}, and Λ was assumed to be log-normally distributed. However, the blood eosinophil count at baseline could not be adequately described by a normal or log normal distribution, for the data were pooled from six studies in healthy volunteers and patients with asthma, with potentially different distributions of baseline eosinophils counts. In addition, no assumption of distribution of baseline eosinophil counts was made, because the raw baseline data were read directly into the model. Therefore, although other random distributions could have been used to describe the variability, they were not evaluated or considered necessary. Instead, for the PD model, the blood eosinophil counts at baseline were directly read in from the dataset with the added residual error component, as was done for the other PD observations (Eq. 9):

$$Eos\,0_i = Eos\,0_{i,O} \cdot e^{\eta \cdot W} \quad (9)$$

where $Eos0_i$ and $Eos0_{i,O}$ represent the predicted and observed baseline blood eosinophil counts for the i^{th} individual, respectively. The random variable η was assumed to be normally distributed with mean 0 and variance of 1. In Eq. 9, W represents the random residual variability to be estimated from nonbaseline observations.[16]

A substantial percentage (59%) of blood eosinophil count data was recorded as "$<$10 cells/μL" in the pooled dataset; to reduce the parameter estimation bias, the PHI function implemented in NONMEM was applied to handle the "$<$10 cells/μL" observations.[17] Because of the adoption of the M3 method to maximize the likelihood of all the data, weighted residuals and conditional weighted residuals were not provided in the NONMEM output. The individual predictions and individual weighted residuals were utilized instead in those plots.

Model evaluation

Model evaluation criteria consisted of inspection of goodness-of-fit plots, bootstrap resampling techniques, and visual predictive checks (VPCs). Internal model evaluation was performed using VPCs, in which the final fixed and random-effect model parameters, along with original dataset as the simulation template, were used to generate median, fifth, and 95th percentiles of 1,000 replicate simulations of the original trials. The simulated BLQ PD data were plot at half lower limit of quantitation for VPCs. The dataset for bootstrapping was resampled a total of 1,000 times and PK and PD parameters were sequentially estimated for each resampled dataset. The median and 95% confidence intervals (CIs) of the bootstrap parameter estimates (based on runs with parameter number of significant figures $\geq$2) were compared with the point estimates of model parameters.

RESULTS

Patient characteristics

Table 1 provides a summary of study designs. **Table 2** lists patient demographics and baseline characteristics. Two of the studies were in male Japanese healthy volunteers ($N = 48$; 100%). Four of the studies were in male ($N = 57$; 37.5%) and female ($N = 95$; 62.5%) patients with asthma, the majority of whom were white ($N = 103$; 67.8%) followed by black ($N = 43$; 28.3%), other ($N = 5$; 3.3%), and Asian ($N = 1$; 0.7%).

Population pharmacokinetics model

Figure 1 provides the structure of the population PK model. The final population PK model was a two-compartment model with first-order elimination from the central compartment, and first-order absorption from the dosing site for s.c. administered benralizumab. The model had IIV for CL, V_c, V_p, k_a, Q, F, and separate residual error variances for s.c. and i.v. administration. The final model parameters are listed in **Table 3**. The estimated CL was 0.323 L/day. The V_c and V_p values were estimated to be 3.16 L and 2.83 L, respectively, suggesting limited extravascular distribution of benralizumab. The absorption of benralizumab from the s.c.

Table 1 Study design and demographics summary

Study description (study #)	Population	No. of participants	Benralizumab route/dosage	Blood sampling schedule	No. of observations	
					Serum benralizumab	Eosinophil count
Phase I, single ascending dose (KHK4563-001)	Healthy Japanese individuals	30	i.v. 0.03–3 mg/kg single dose	PK: intensive up to day 84 PD: predose, 6 h, and up to day 84	492	355
Phase I, single ascending dose (KHK4563-002)	Healthy Japanese individuals	18	s.c. 25, 100, 200 mg single dose	PK: intensive up to day 84 PD: predose, 6 h, and up to day 84	252	216
Phase I, single ascending dose (MI-CP158)	Adults w/asthma, USA	44	i.v. 0.0003–3 mg/kg single dose	PK: intensive up to day 84 PD: predose and days 1, 2, 7, 58, and 84	553	552
Phase I, randomized, double-blind, placebo-controlled dosage-increase (MI-CP166)	Adults w/asthma, USA	17	i.v. 1 mg/kg single dose (cohort 1) s.c. 100 or 200 mg every 4 weeks × 3 (cohort 2)	Cohort 1: PK/PD sampling up to day 84 Cohort 2: PK/PD sampling up to day 140	125	143
Phase II, randomized, double-blind, placebo-controlled (MI-CP186)	Adults w/asthma, USA	72	i.v. 0.3 or 1 mg/kg single dose	PK: predose, 1 h, and days 7, 42, and 84 PD: predose and days 7, 42, and 84	257	217
Phase II, randomized, double-blind, placebo-controlled dosage increase (MI-CP197)	Adults w/asthma, USA	19	s.c. 25, 100, or 200 mg every 4 weeks × 3	PK: predose and days 1, 7, 28, 35, 56, 84, 112, and 161 PD: predose and days 1, 7, 28, 56, 84, 112, and 161	141	181

PD, pharmacodynamics; PK, pharmacokinetics.

dosing site was relatively slow, with an estimated k_a of 0.252 day^{-1} (mean absorption time of 3.97 days) and F of 52.6%. There was greater additive residual error for the s.c. group compared with the i.v. group.

Body weight was identified as a clinically relevant covariate affecting CL, V_c, and V_p (**Figure 2**). The exponent for the impact of body weight on CL was not significantly different from a typical value of 0.75 for a mAb. Thus, this parameter was fixed at 0.75 in the final model. Race was a significant factor for V_c, with Japanese healthy volunteers having a larger V_c than non-Japanese patients with asthma (**Figure 2**). Of 19 patients with detectable ADAs to benralizumab, 11 had presence of high-titer ADA ($\geq$400) and elevated CL. Age, sex, and tobacco smoking history had no apparent impact on the PK of benralizumab in healthy volunteers or patients with asthma.

Table 2 Summary of demographics and baseline covariates

Variables	Japanese i.v. ascending dose (KHK4563-001)	Japanese s.c. ascending dose (KHK4563-002)	USA asthma i.v. ascending dose (MI-CP158)	USA asthma i.v. and s.c. dosage increase (MI-CP166)	USA asthma phase II (MI-CP186)	USA asthma phase II (MI-CP197)	Total
Sex, M/F	30/0	18/0	17/27	7/10	25/47	8/11	105/95
Race, W/A/B/O[a]	0/30/0/0	0/18/0/0	41/0/1/2	16/0/1/0	30/1/38/3	16/0/3/0	103/49/43/5
Age, years[b]	29.1 ± 6.43 (20–39)	25.6 ± 5.38 (20–37)	24.7 ± 6.03 (18–41)	38.9 ± 13.8 (20–62)	36.3 ± 10.8 (19–60)	45.6 ± 12.8 (27–69)	32.8 ± 11.5 (18–69)
BMI, kg/m^2	21.6 ± 1.73 (18.8–24.3)	21.6 ± 1.83 (18.7–24.8)	24.5 ± 3.53 (17.8–32.6)	28.4 ± 6.13 (21.1–45.6)	30.4 ± 8.16 (18.2–51.6)	29.4 ± 5.94 (20.8–44.5)	26.8 ± 6.83 (17.8–51.6)
Body weight, kg[b]	65.0 ± 6.21 (54.7–77.6)	63.7 ± 7.09 (52.7–76.3)	72.4 ± 12.0 (51.6–108)	79.7 ± 16.6 (57.5–109)	85.5 ± 22.9 (42–136.1)	84.7 ± 20.1 (51.7–130.6)	77.0 ± 19.0 (42–136.1)
Baseline eosinophil count, cells/mL[b]	0.2 ± 0.16 (0.01–0.68)	0.2 ± 0.12 (0.03–0.4)	0.3 ± 0.17 (0.01–0.72)	0.3 ± 0.22 (0.1–0.9)	0.2 ± 0.6 (0–4.53)	0.3 ± 0.22 (0.05–1)	0.24 ± 0.37 (0.005–4.53)
Smoking status, U/C/P/N[c]	30/0/0/0	18/0/0/0	44/0/0/0	0/0/3/14	0/21/18/33	0/0/5/14	92/21/26/61

A, Asian; ADAs, antidrug antibodies; B, black; BMI, body mass index; O, other; W, white.
[a]Displayed as white/Asian/black/other.
[b]Continuous covariates are displayed as mean ± SD (min–max); numbers of patients are given for categorical covariates.
[c]Displayed as unknown/current/past/nonsmoker.

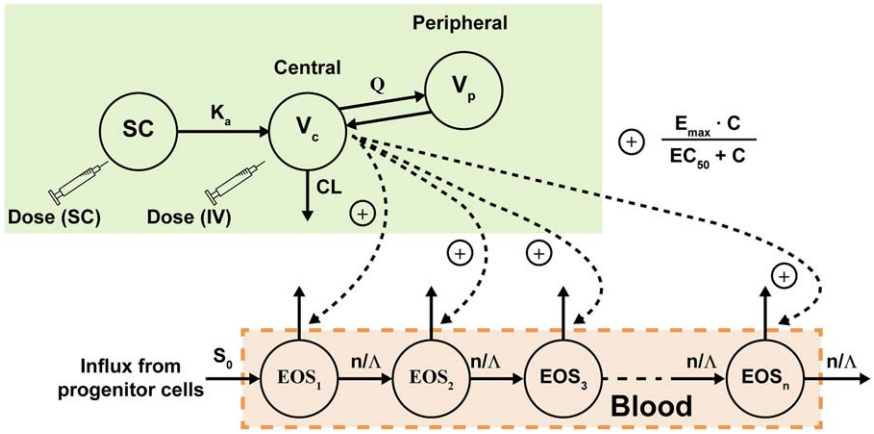

Figure 1 Schematic of the pharmacokinetic/pharmacodynamic (PK/PD) model of benralizumab. EOS, eosinophils in peripheral blood; C, concentration; CL, clearance; EC_{50}, half-maximal effective concentration; E_{max}, maximal rate of eosinophil depletion by benralizumab; k_a, first-order absorption rate constant; Λ, lifespan of blood eosinophils; Q, intercompartmental (distribution) clearance; S_0, influx rate of eosinophils; SC, subcutaneous; V_c, volume of distribution for the central compartment; V_p, volume of distribution for the peripheral compartment.

The IIVs of s.c. absorption parameters of benralizumab, 53% and 32% coefficient of variation (%CV) for k_a and F, respectively, were greater than those of disposition parameters (23–33%CV). The estimated proportional residual error was close to the 15% CV precision requirement for assay validation. However, the estimated additive residual error was greater for the s.c. cohorts (SD 36 ng/mL) than the i.v. cohorts (SD 7.0 ng/mL), suggesting more complex s.c. absorption than a first-order process as assumed in the PK model.

Table 3 Final population pharmacokinetics model parameter estimates.

Parameter	Population estimate	Bootstrap[a]	
		Median	95% CI
CL, L/d	0.323	0.323	0.309–0.339
Weight on CL[b]	0.75 (FIX)	0.75	-
ADAs on CL[c]	1.52	1.51	1.19–1.63
V_c, L	3.16	3.16	2.96–3.36
Weight on V_c[b]	0.651	0.652	0.434–0.916
Race, Japanese HVs on V_c, fraction	1.34	1.33	1.22–1.46
Q, L/d	0.939	0.938	0.818–1.09
V_p, L	2.83	2.85	2.64–3.04
Weight on V_p[b]	0.576	0.563	0.292–0.858
k_a, d^{-1}	0.252	0.253	0.211–0.302
F	0.526	0.527	0.472–0.591
IIV			
η_{CL}, %CV	24.9	24.8	21.3–28.6
η_{Vc}, %CV	23.1	22.9	18.3–27.2
η_{Q}, %CV	28.5	28.4	10.6–59.1
η_{Vp}, %CV	32.7	32.0	25.7–39.2
η_{ka}, %CV	52.7	49.9	29.4–70.4
η_{F}, %CV	32.4	31.5	20.9–40.8
Residual variability			
Proportional error s.c., %CV	14.2	14.1	11.4–16.6
Additive error s.c., SD, ng/mL	35.6	35.0	19.3–65.1
Proportional error i.v., %CV	13.3	13.3	11.4–14.9
Additive error i.v., SD, ng/mL	7.02	6.89	4.56–9.81

ADAs, anti-drug antibodies; CI, confidence interval; CL, clearance; CV, coefficient of variation; F, bioavailability; HV, healthy volunteer; IIV, interindividual variability; k_a, absorption rate constant; Q, intercompartmental clearance; V_c, volume of distribution of the central compartment; V_p, volume of distribution of the peripheral compartment.
[a]Based on 743 runs with parameter significant digits ≥2 (of 1,000 bootstrap runs). [b]Allometric exponent. [c]Natural exponent.

The observed and predicted benralizumab concentrations were distributed along a line of unity, and there was no apparent bias in the basic goodness-of-fit plots for the final PK model (**Supplementary Figure S1**). The median and 95% CI of the 1,000 bootstrapping estimates for the benralizumab PK parameters matched the final model PK parameter estimates, indicating robustness of the final PK model (**Table 3**). The simulated VPCs for the single-ascending-dose study in patients with asthma matched the observed benralizumab concentrations (**Figure 3a, b**). These data confirm that the model adequately describes the benralizumab PK data.

Pharmacokinetics/pharmacodynamics model

Blood cell kinetics is frequently depicted by a hematopoietic transit model.[14,15,18] A model with ADCC induced by benralizumab was constructed to describe the PD effect on blood eosinophils. In **Figure 1**, each transit compartment represents eosinophils in the i^{th} age compartment. The total blood eosinophil count (Eos_{total}) is the sum of eosinophils in all of the transit compartments. The number of aging compartments, *n*, was set to five to adequately describe the variance of eosinophil life span. Because of the enhanced ADCC activity of benralizumab, many blood eosinophil count data were recorded as <10 cells/μL upon benralizumab administration. The PD observations that were BLQ were analyzed using a likelihood-based M3 method.[17] The estimated population PD parameters and random effects are provided in **Table 4**. The lifespan (Λ) of circulating eosinophils in blood was fixed at 2.64 days, corresponding to a half-life of 44 hours.[19] The EC_{50} was 82.7 ng/mL, and the maximal rate of

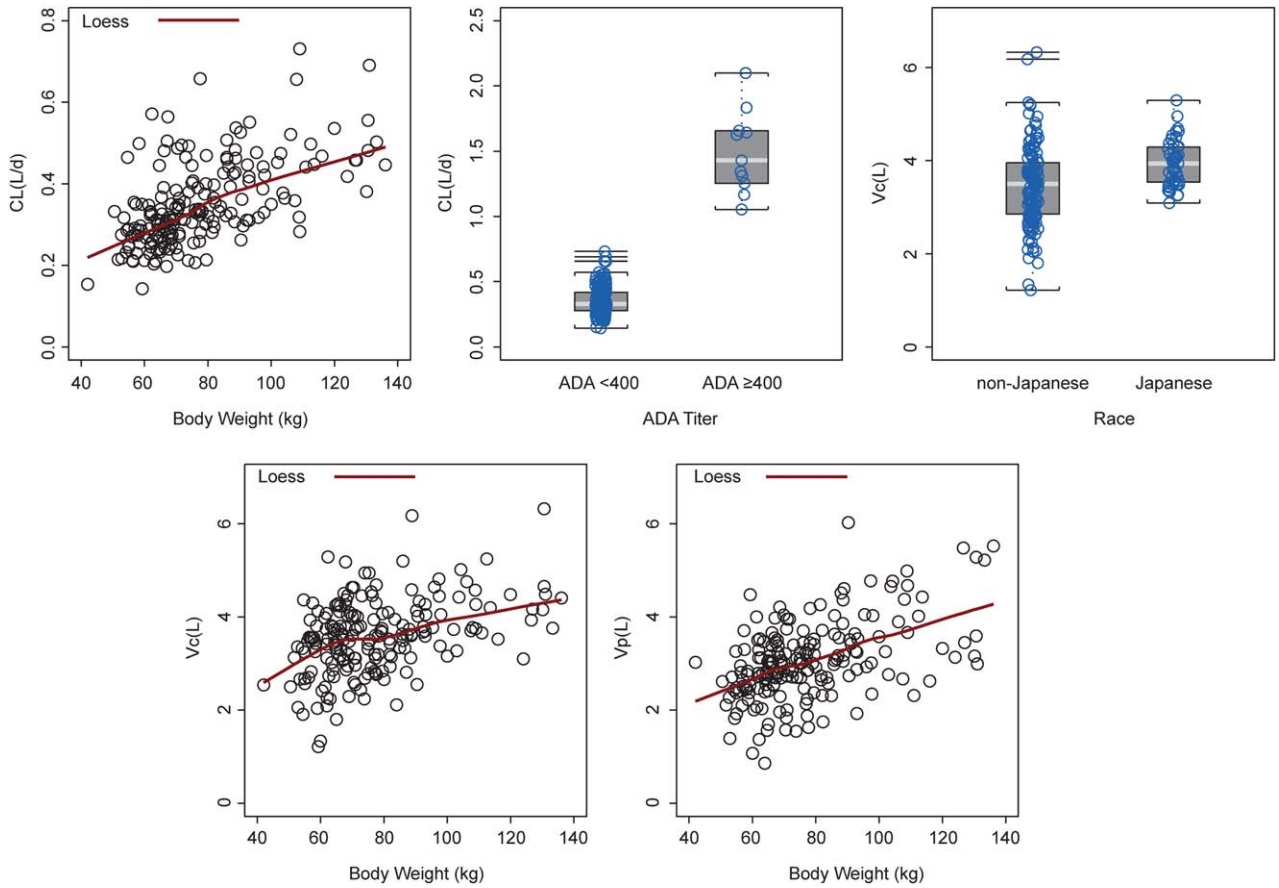

Figure 2 Effect of body weight, antidrug antibodies (ADAs), and race on clearance (CL), volume of distribution of the central compartment (V_c), and volume of distribution of the peripheral compartment (V_p) of benralizumab; each open circle represents one individual study participant.

eosinophil depletion by benralizumab (E_{max}) was 18.8 day^{-1} (mean eosinophil residence time of 0.053 days, or 1.28 hours, in the presence of excess benralizumab).

The median and 95% CI of the 1,000 bootstrapping estimates for the benralizumab PD parameters matched the final model PD parameter estimates, indicating robustness of the PD model (**Table 4**). **Figure 3c** presents the VPC plots for a single-ascending-dose study in patients with asthma. The VPCs confirmed that the model adequately described the eosinophil count data.

DISCUSSION

In humans, IL-5 plays a key role in the maturation, growth, and activity of eosinophils.[7,8] Depletion of blood eosinophils has significantly reduced the exacerbation rate for patients with uncontrolled asthma.[20–22] Unlike other anti-IL-5 mAbs, benralizumab targets IL-5R expressed on eosinophils and induces cell apoptosis by enhancing ADCC function.[10] In early-stage clinical studies, benralizumab treatment resulted in substantial and prolonged depletion of blood eosinophil count. In a first-in-human study, the dosages of benralizumab were decreased to as low as 0.003 and 0.0003 mg/kg to identify a dosage threshold for blood eosinophil depletion.[11] To facilitate the clinical development of benralizumab, we conducted PK/PD modeling and simulations at every stage of development to integrate data collected from prior trials and to predict the eosinophil response in patients for future studies. To support the rational selection of an appropriate dosage regimen for a proof-of-concept, phase IIb study in patients with severe, uncontrolled asthma, PK, and blood eosinophil count data collected from six phase I and IIa studies were pooled and simultaneously modeled with a population approach.

Typically, mAbs targeting membrane-bound receptors are subject to target-mediated disposition, or antigen-sink effect, resulting in accelerated systemic clearance at low concentrations.[23–27] Although benralizumab targets a membrane receptor, IL-5Rα, its PK profile demonstrated no evidence of nonlinearity even at dosages as low as 0.03 mg/kg in humans.[11] From the population modeling in our study, benralizumab PK was adequately described by a two-compartment model with a first-order elimination pathway from the central compartment. The dose-proportional PK for benralizumab is likely associated with rapid depletion of the target receptor pool (eosinophils) in the blood following benralizumab administration. The estimated systemic CL for benralizumab, at 0.323 L/day, is within the range for therapeutic mAbs.[28] The estimated distribution volumes

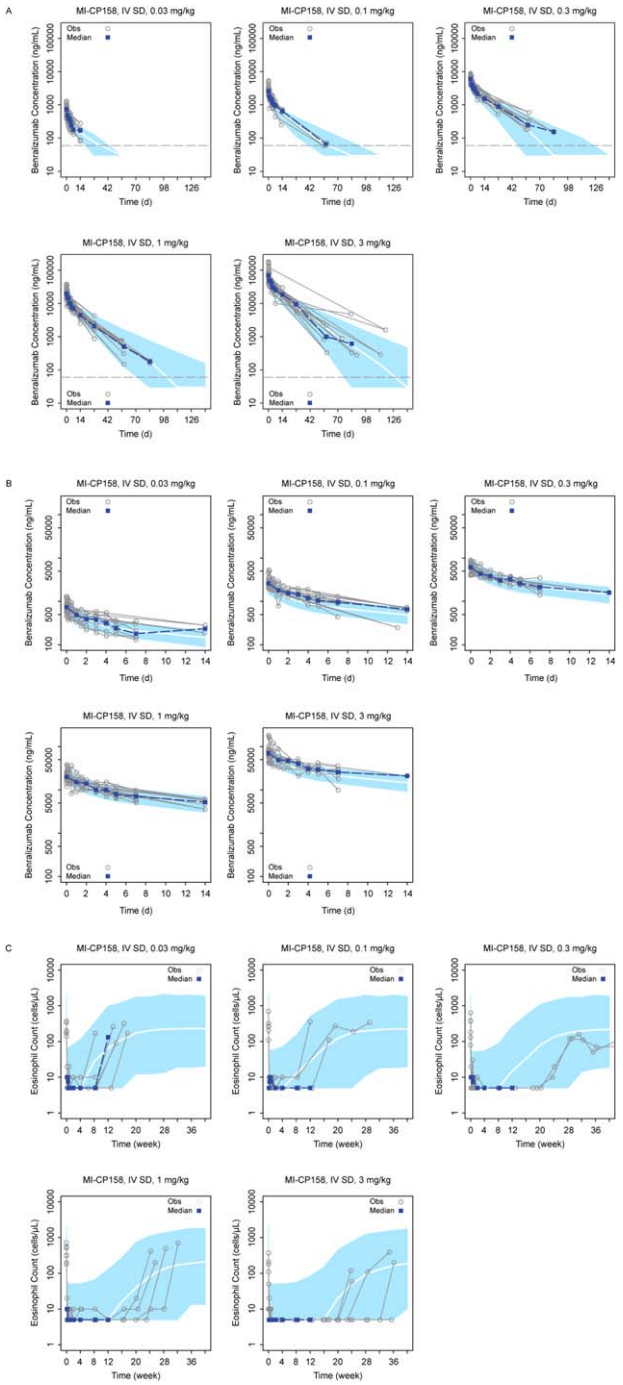

Figure 3 (**a**) Visual predictive check (VPC) for benralizumab concentrations from the first-in-human single-ascending-dose study (MI-CP158); solid curve: median of simulated profiles; shaded area: region between the fifth and 95th percentiles. The horizontal dashed line represents the lower limit of quantitation. IV, intravenous; SD, single dose. (**b**) Is **Figure 3a** focused on the initial 14 days. (**c**) VPC for blood eosinophil count from the first-in-human single-ascending-dose study (MI-CP158; 6–9 patients per cohort); solid curve: median of simulated profiles; shaded area: region between the fifth and 95th percentiles. IV, intravenous; SD, single dose. Only patients with fully depleted eosinophils were followed beyond week 12 for the safety assessment in this study.

Table 4 Final population pharmacodynamics model parameter estimates

Parameter	Population estimate	Bootstrap[a]	
		Median	95% CI
E_{max}, d^{-1}	18.8	18.8	14.9–22.3
EC_{50}, ng/mL	82.7	82.7	63.7–87.8
Life span [Λ], d	2.64 FIX		
IIV			
η_{Emax}, %CV	41.0	41.0	36.2–51.4
η_{EC50}, %CV	40.6	40.6	37.2–55.0
η_{Λ}, %CV	50.4	50.4	48.1–69.4
Residual variability			
Proportional error, %CV	76.6	76.6	64.6–84.6

CI, confidence interval; CV, coefficient of variation; EC_{50}, half-maximal effective concentration; E_{max}, maximal rate of eosinophil destruction by benralizumab; IIV, interindividual variability.
[a]Based on 950 runs with parameter significant digits ≥2 (of 1,000 bootstrap runs).

(V_c and V_p) of benralizumab were typical for IgG. Following s.c. administration, mAbs are absorbed through the lymphatic system. This process involves convective flow of interstitial fluid, which drains slowly into the systemic circulation.[29] The mean absorption time of s.c. administered benralizumab was 3.97 days ($k_a = 0.252$ d^{-1}), similar to data reported for therapeutic mAbs.[28]

In the absence of target-mediated clearance, the elimination of therapeutic IgGs takes place primarily through the reticuloendothelial system.[29] Distribution of IgG and other recombinant proteins is usually restricted to extracellular fluid.[29] As expected from covariate analysis, the systemic CL as well as distribution volume of benralizumab increased with body weight. No difference in CL between Japanese and non-Japanese patients was identified. However, the estimated V_c was 34% greater for Japanese healthy volunteers than for non-Japanese patients with asthma of the same body weights. Eosinophil counts for healthy volunteers were much lower than for patients with asthma. There was no obvious explanation for the race impact on V_c. If benralizumab's binding to target cells in blood had any impact on benralizumab PK, the observed C_{max} following i.v. administration would have been greater in healthy volunteers (i.e., smaller V_c). The race impact on V_c could have been a spurious observation because of the small sample size. Nevertheless, the estimated individual V_c mostly overlapped between Japanese healthy volunteers and non-Japanese patients with asthma. In addition, race had no impact on CL and overall drug exposure. The racial difference in V_c is not considered clinically relevant. The potential impact of race on benralizumab PK will undergo further evaluation upon completion of phase III clinical trials with greater sample sizes.

Some serum samples tested positive for the presence of ADAs, and reduced PK exposure was observed in those individuals with high-titer ADAs. From population analysis, the development of ADAs with titers ≥400 elevated the CL of benralizumab by a factor of ~4.6-fold. Given the small number of individuals with high-titer ADAs and the short duration of early-stage clinical studies, the incidence and impact of ADAs on benralizumab PK and PD need to be further evaluated in

late-stage clinical trials. Age, sex, and tobacco-smoking history had no apparent effect on the PK of benralizumab in humans.

Benralizumab is an afucosylated IgG_1 κ mAb with enhanced ADCC activity. In healthy volunteers and patients with asthma, benralizumab treatment resulted in rapid, substantial, and prolonged depletion of blood eosinophil counts. Many PD observations were recorded as <10 cells/μL because the absolute counts fell below the lower assay threshold. Such BLQ PD observations posed a challenge for proper data analysis, for ignoring or setting the value to half the lower limit of quantitation resulted in data fitting difficulty (nonconvergence) or parameter estimation bias. This situation differs from the analysis of BLQ PK observations, in which the monotonic PK declining phase prior to BLQ observations helps to anchor (extrapolate) the individual disposition curves. For PD modeling, these BLQ PD data will eventually recover and become quantifiable after PK and treatment effects diminish. In this effort, the PHI function implemented in NONMEM previously used for the proper analysis of BLQ PK observations[17] was adopted to handle the BLQ eosinophil count observations following benralizumab treatment. The use of the likelihood-based M3 method stabilized the model and enabled proper estimation of PD structural and variance parameters.

Depletion of blood eosinophils by benralizumab was depicted by accelerated target cell depletion in each aging compartment of a hematopoietic transit model.[14,18] To avoid model overparameterization, the eosinophil lifespan was fixed at 2.64 days ($t_{1/2} = 44$ hours) as determined with Cr^{51}-labeled eosinophils in patients with idiopathic hypereosinophilic syndrome.[19] The estimated maximum increase in eosinophil depletion as induced by benralizumab was $\sim$50-fold over normal senescence rate. When the serum concentration of benralizumab was much greater than EC_{50} (82.7 ng/mL), the mean residence time of eosinophils in blood was estimated to be $\sim$1.3 hours.

Most eosinophils reside in tissues with epithelial surfaces exposed to external environments (gastrointestinal tract, lungs, and skin), and tissue eosinophils are capable of returning to the circulating blood and bone marrow after entering the tissues.[30] Tracer kinetic studies using radiolabeled eosinophils demonstrated transient disappearance of infused eosinophils followed by re-emergence and subsequent decline of eosinophils in blood.[19] Closer examination of individual eosinophil profiles in a single-ascending-dose study also revealed a complex pattern of blood eosinophil count suppression by benralizumab: a rapid initial declining phase followed by a shallow "shoulder," and then more substantial and prolonged depletion of eosinophil counts. The initial decline is likely the result of the instant benralizumab binding and elimination of circulating eosinophils in the blood by ADCC. The subsequent leveling could be because of either the migration of eosinophils from tissues to blood or enhanced production of *de novo* eosinophil production. During the third phase, more substantial depletion of blood eosinophil counts may reflect the continuing removal of tissue eosinophils or eosinophil precursor cells by benralizumab.

Various eosinophil models were constructed to depict the "shouldering" phenomenon, including the reduction of eosinophil influx (*de novo* production) by benralizumab, transient expansion of blood eosinophil distribution volume, and addition of a peripheral tissue compartment for eosinophils. However, none of these efforts significantly improved the overall fit of the data or resulted in reliable parameter estimates. The complex suppression pattern of the blood eosinophil count was not observed in other clinical studies because of greater dosages and/or less frequent blood sampling schedules. In addition, the primary PD activity and therapeutic efficacy of benralizumab are associated with the later phase of eosinophil depletion. As such, the PD modeling focused on the overall longitudinal profile of blood eosinophil count, and no further attempt was made to model the transient leveling off the blood eosinophil count prior to the more prolonged depletion.

Based on the simulated eosinophil profiles using this PK/PD model, three dosages and an every-8-week dosing interval were selected for efficacy assessment in a proof-of-concept phase IIb study in patients with uncontrolled asthma. The outcome of the study was in line with projections.[21] Further exposure-response analysis of primary and two secondary efficacy endpoints from the proof-of-concept study identified the optimal dosing regimen for benralizumab phase III pivotal trials.[31]

In summary, population meta-analysis demonstrated dose-proportional PK of benralizumab. Systemic CL and distribution volumes of benralizumab increased with body weight. The impact of race on V_c, as identified from covariate analysis, is not considered clinically relevant. High-titer ADAs were associated with elevated CL of benralizumab. A transit hematopoietic model in which benralizumab induces eosinophil depletion in each aging compartment adequately described the blood-eosinophil count response in humans. Use of the M3 method (PHI function in NONMEM) facilitated proper handling of unquantifiable PD observations upon benralizumab dosing. The PK/PD modeling results enabled appropriate selection of three dosages and an every-8-week dosing schedule to be further evaluated in a proof-of-concept, phase IIb study in patients with uncontrolled asthma.[32]

Acknowledgments. Susan K. Paulson, PhD, of Paulson PK Consulting, LLC, assisted with the first draft of this manuscript. Editorial assistance was provided by Sophie Walton, MSc, of QXV Comms (an Ashfield business, part of UDG Healthcare PLC), Alan Saltzman, of Endpoint Medical Communications (Conshohocken, PA), and Michael A. Nissen, ELS, of AstraZeneca (Gaithersburg, MD). This support was fully funded by AstraZeneca.

Conflict of Interest. B.W., L.Y., and L.R. are employees of MedImmune LLC (Mountain View, California, and Gaithersburg, Maryland). Z.Y. was an employee of MedImmune when the data analysis was conducted. This study was funded by MedImmune.

Author Contributions. B.W. and L.Y. contributed equally to this work. B.W., Z.Y., and L.R. were involved in the study design. B.W., L.Y., Z.Y., and L.R. were involved in the data analysis and interpretation.

1. Takatsu, K., Takaki, S. & Hitoshi, Y. Interleukin-5 and its receptor system: implications in the immune system and inflammation. *Adv. Immunol.* **57**, 145–190 (1994).

2. Molfino, N.A., Gossage, D., Kolbeck, R., Parker, J.M. & Geba, G.P. Molecular and clinical rationale for therapeutic targeting of interleukin-5 and its receptor. *Clin. Exp. Allergy* **42**, 712–737 (2012).
3. Ochensberger, B., Tassera, L., Bifrare, D., Rihs, S. & Dahinden C.A. Regulation of cytokine expression and leukotriene formation in human basophils by growth factors, chemokines and chemotactic agonists. *Eur. J. Immunol.* **29**, 11–22 (1999).
4. Murata, Y., Takai, S., Migita, M., Kikuchi, Y., Tominaga, A. & Takatsu, K. Molecular cloning and expression of the human interleukin 5 receptor. *J. Exp. Med.* **175**, 341–351 (1992).
5. Migita, M. *et al.* Characterization of the human IL-5 receptors on eosinophils. *Cell Immunol.* **133**, 484–497 (1991).
6. Walsh, G.M., Sexton, D.W. & Blaylock, M.G. Corticosteroids, eosinophils and bronchial epithelial cells: new insights into the resolution of inflammation in asthma. *J. Endocrinol.* **178**, 37–43 (2003).
7. Ilmarinen, P. & Kankaanranta, H. Eosinophil apoptosis as a therapeutic target in allergic asthma. *Basic Clin. Pharmacol. Toxicol.* **114**, 109–117 (2014).
8. Mukherjee, M., Sehmi, R. & Nair, P. Anti-IL5 therapy for asthma and beyond. *World Allergy Organ. J.* **7**, 32 (2014).
9. Koike, M. *et al.* Establishment of humanized anti-interleukin-5 receptor alpha chain monoclonal antibodies having a potent neutralizing activity. *Hum. Antibodies* **18**, 17–27 (2009).
10. Kolbeck, R. *et al.* MEDI-563, a humanized anti-IL-5 receptor α mAb with enhanced antibody-dependent cell-mediated cytotoxicity function. *J. Allergy Clin. Immunol.* **125**, 1344–1353 (2010).
11. Busse, W.W. *et al.* Safety profile, pharmacokinetics, and biologic activity of MEDI-563, an anti-IL 5 receptor α antibody, in a phase I study of subjects with mild asthma. *J. Allergy Clin. Immunol.* **125**, 1237–1244 (2010).
12. Efficacy and safety study of benralizumab in adults and adolescents inadequately controlled on inhaled corticosteroid plus long-acting β2 agonist. <https://clinicaltrials.gov/ct2/show/NCT01914757?term=NCT01914757&rank=1> (2016). Accessed 13 April 2016.
13. Zhang, L., Beal, S.L. & Sheiner, L.B. Simultaneous vs. sequential analysis for population PK/PD data I: best-case performance. *J. Pharmacokinet. Pharmacodyn.* **30**, 387–404 (2003).
14. Harker, L.A. *et al.* Effects of megakaryocyte growth and development factor on platelet production, platelet life span, and platelet function in healthy human volunteers. *Blood* **95**, 2514–2522 (2000).
15. Wang, B. *et al.* Pharmacokinetic and pharmacodynamics comparability study of moxetumomab pasudotox, an immunotoxin targeting CD22, in cynomolgus monkeys. *J. Pharm. Sci.* **102**, 250–261 (2013).
16. Dansirikul, C., Silber, H.E. & Karlsson, M.O. Approaches to handling pharmacodynamic baseline responses. *J. Pharmacokinet. Pharmacodyn.* **35**, 269–283 (2008).
17. Ahn, J.E., Karlsson, M.O., Dunne, A. & Ludden, T.M. Likelihood based approaches to handling data below the quantification limit using NONMEM VI. *J. Pharmacokinet. Pharmacodyn.* **35**, 401–421 (2008).
18. Krzyzanski, W. Interpretation of transit compartments pharmacodynamic models as lifespan based indirect response models. *J. Pharmacokinet. Pharmacodyn.* **38**, 179–204 (2011).
19. Dale, D.C., Hubert, R.T. & Fauci, A. Eosinophil kinetics in the hypereosinophilic syndrome. *J. Lab. Clin. Med.* **87**, 487–495 (1976).
20. Castro, M. *et al.* Reslizumab for inadequately controlled asthma with elevated blood eosinophil counts: results from two multicentre, parallel, double-blind, randomised, placebo-controlled, phase 3 trials. *Lancet Respir. Med.* **3**, 355–366 (2015).
21. Castro, M. *et al.* Benralizumab, an anti-interleukin 5 receptor α monoclonal antibody, versus placebo for uncontrolled eosinophilic asthma: a phase 2b randomised dose-ranging study. *Lancet Respir. Med.* **2**, 879–890 (2014).
22. Ortega, H.G. *et al.* Mepolizumab treatment in patients with severe eosinophilic asthma. *N. Engl. J. Med.* **371**, 1198–1207 (2014).
23. Bauer, R.J., Dedrick, R.L., White, M.L., Murray, M.J. & Garovoy, M.R. Population pharmacokinetics and pharmacodynamics of the anti-CD11a antibody hu1124 in human subjects with psoriasis. *J. Pharmacokinet. Biopharm.* **27**, 397–420 (1999).
24. Hayashi, N., Tsukamoto, Y., Sallas, W.M. & Lowe, P.J. A mechanism-based binding model for the population pharmacokinetics and pharmacodynamics of omalizumab. *Br. J. Clin. Pharmacol.* **63**, 548–561 (2007).
25. Wang, B. *et al.* Pharmacogenomics and translational simulations to bridge indications for an anti-interferon-α receptor antibody. *Clin. Pharmacol. Ther.* **93**, 483–492 (2013).
26. Wang, B. *et al.* Mechanistic modeling of antigen sink effect for mavrilimumab following intravenous administration in patients with rheumatoid arthritis. *J. Clin. Pharmacol.* **52**, 1150–1161 (2012).
27. Mager, D.E. & Jusko, W.J. General pharmacokinetic model for drugs exhibiting target-mediated drug disposition. *J. Pharmacokinet. Pharmacodyn.* **28**, 507–532 (2001).
28. Dirks, N.L. & Meibohm, B. Population pharmacokinetics of therapeutic monoclonal antibodies. *Clin. Pharmacokinet.* **49**, 633–659 (2010).
29. Lobo, E.D., Hansen, R.J. & Balthasar, J.P. Antibody pharmacokinetics and pharmacodynamics. *J. Pharm. Sci.* **93**, 2645–2668 (2004).
30. Kita, H. & Bochner, B.S. Biology of eosinophils. In *Allergy Principles and Practice.* 5th edn. 242–260 (Mosby, St. Louis, MO, 1998).
31. Wang, B., *et al.* Exposure-response analysis for determination of benralizumab optimal dosing regimens in adults with asthma. *Am. J. Respir. Crit. Care Med.* **189**, A1324 (2014).
32. Study to evaluate the efficacy and safety of MEDI-563 in adults with uncontrolled asthma. <https://clinicaltrials.gov/ct2/show/NCT01238861?term=NCT01238861&rank=1> (2014). Accessed 13 April 2016.

Supplementary information accompanies this paper on the *CPT: Pharmacometrics & Systems Pharmacology* website (http://www.psp-journal.com)